Role of the scrape-off layer in the type I ELM dynamics in AUG and TCV

L. Frassinetti[1], M. G. Dunne[2], U. Sheikh[3], F. Orain[2], M. Bernert[2], G. Birkenmeier[2], P. Blanchard[3], D. Carralero[2], M. Cavedon[2], S. Coda[3], R. Fischer[2], M. Hoelzl[2], F. Laggner[4], R. M. McDermott[2], H. Meyer[5], A. Merle[3], C. Theiler[3], K. Verhaegh[3] E. Viezzer[2], E. Wolfrum[2], the ASDEX Upgrade Team[2], the TCV Team[3] and the EUROfusion MST1 Team[*].

[1]Division of Fusion Plasma Physics, KTH Royal Institute of Technology, Stockholm SE
[2]Max-Planck-Institut für Plasma Physik, Boltzmannstr.2, 85748 Garching, Germany
[3]Ecole Polytechnique Fédérale de Lausanne (EPFL), Swiss Plasma Center (SPC), Lausanne, Switzerland
[4]Institute of Applied Physics, TU Wien, Fusion@ÖAW, 1040 Vienna, Austria
[5]CCFE, Culham Science Centre, Abingdon, Oxon OX14 3DB, UK
*see the author list of Meyer et al, Overview of progress in European Medium Sized Tokamaks towards an integrated plasma-edge/wall solution, accepted in Nuclear Fusion

INTRODUCTION

Recent results from the metal wall machines JET-ILW [1] and AUG [2,3] have shown that the fast collapse of the pedestal energy during an ELM (time scale <1ms) can be followed by a second collapse characterized by a longer time scale (≈2-5ms). Experimental results show that the second collapse tends to disappear when nitrogen is seeded [1,2,3] and/or good confinement is achieved [4]. These observations, due to the fact that N seeding leads to the increase of the electron pedestal temperature T_e^{ped} [5,6,7] might suggest that the presence of the second collapse is correlated to low T_e^{ped}. More recently, an empirical correlation between the pre-ELM divertor temperature (T_{div}) and the energy losses of the second collapse has been observed in AUG [3]. This has suggested that the divertor and/or the scrape-off layer conditions can play a role in the ELM dynamics, as also noted in [2,4]. To date, the origin of the second collapse is not clear yet and several questions are still open:

- is the second collapse correlated to T_e^{ped} or to the pedestal pressure or to any pedestal plasma parameter related to the temperature (such as resistivity or collisionality)?
- can the second collapse disappear only when the seeded species is nitrogen?
- is the presence of the second collapse correlated to the divertor and/or SOL conditions?

This work will try to answer these questions by investigating the ELM behavior in AUG and TCV for plasmas in which nitrogen and neon have been seeded and in deuterium fuelling scans.

NEON SEEDING IN AUG

Previous AUG results have shown that the nitrogen seeding leads to the increase of T_e^{ped} with no significant effect on the electron pedestal density n_e^{ped} [7]. Above a specific rate of nitrogen (and consequently at sufficiently high T_e^{ped}), the second collapse disappears [3]. In this section, instead, the effect of neon seeding is discussed. Figure 1 shows an AUG shot in which only neon is seeded while the other engineering parameters (including power and main gas rate) are kept constant [figure 1(a)]. The neon leads to an increase in n_e^{ped} while no major effect on T_e^{ped} is observed [figure 1(b)]. In the last part of the discharge, when the neon rate and n_e^{ped} are high, the second collapse disappears. In figure 1(c), the ELMs characterized by the second collapse are highlighted in black (hereafter labelled as "*long ELMs*" for

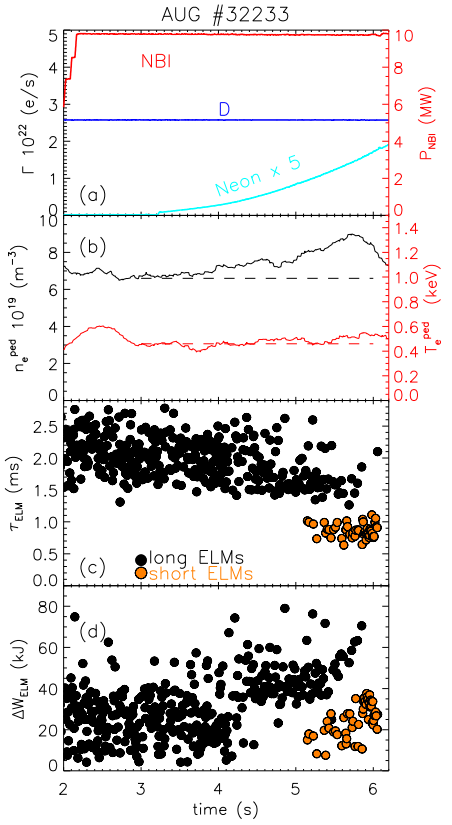

Figure 1. Time evolution of (a) NBI power, deuterium rate and neon rate, (b) n_e^{ped} (measured from TS) and T_e^{ped} (measured from ECE), (c) ELM duration and (d) ELM energy losses.

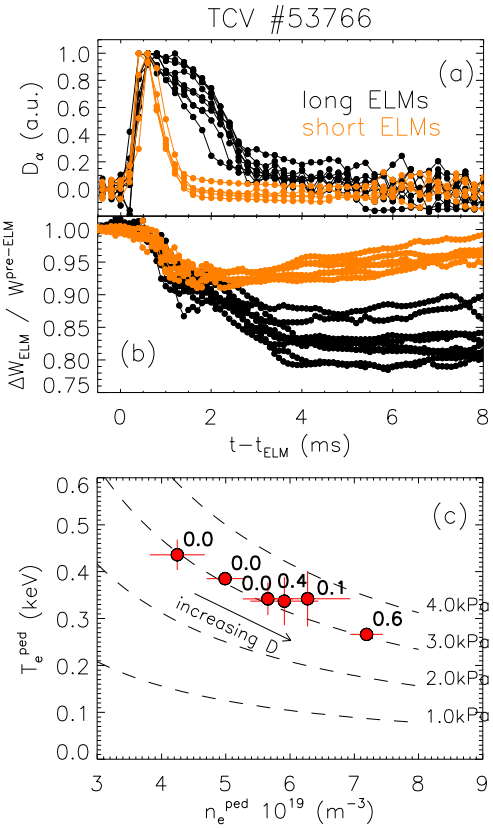

Figure 2. ELM synchronized time evolution of (a) D_α and (b) energy losses. (c) Correlation of T_e^{ped} and n_e^{ped}.for a D fuelling scan in TCV. The bold numbers highlight the fraction of long ELMs.

simplicity) while those characterized by only the first collapse are in orange (and hereafter labelled "*short ELMs*"). The separation between the ELMs characterized by only the first collapse and those followed by the second collapse is clear in terms of both ELM duration and ELM energy losses. The ELM duration (τ_{ELM}), quantified by calculating the full width half maximum of the divertor current [3], is shown in figure 1(c). The ELM energy losses have been estimated from the drop in W_{MHD} and are shown in figure 1(d).
The results obtained with neon seeding shows that T_e^{ped} is not a parameter directly relevant to the presence of the second collapse.

DEUTERIUM FUELLING SCAN IN TCV

The second collapse has been observed also in TCV H-mode plasmas. An example for a NBH heated plasma (1MW) at I_p=210kA is shown in figure 2. Figure 2(a) shows the D_α time traces for all the ELMs of the discharge. The time traces have been synchronized in order to have at t=0 the ELM onset. Figure 2(b) shows the relative ELM energy losses estimated from the diamagnetic signal. For ≈60% of the ELMs, the first collapse ($\Delta W_{ELM}/W \approx 10\%$) is followed by a second collapse which produces further energy losses ($\Delta W_{ELM}/W \approx 20\%$).
Figure 2(c) summarizes the results of a deuterium fuelling scan with no impurity seeding. The increase of the D rate fuels the plasma leading to higher n_e^{ped} but does not affect p_e^{ped}. The bold numbers in figure 2(c) show the ratio between the number of long ELMs (*i.e.* those

followed by the second collapse) over the total number of ELMs. The second collapse is present only at high density / high D fuelling. The result shows that the presence of the second collapse is not directly related to the pedestal pressure.

CHARACTERIZATION OF THE PRE-ELM DIVERTOR TEMPERATURE.

The correlation between the pre-ELM divertor temperature T_{div} and the energy losses for the ELMs characterized by the second collapsed was already observed in AUG [3]. However, no correlation between the presence of the second collapse and T_{div} was discussed. Figure 3(a) shows T_{div} measured by the AUG Langmuir probes for the shot shown in figure 1 during a time interval when both long and short ELMs are present. The data are averaged in a time window -0.3ms to -0.1ms before the ELMs. The pre-ELM T_{div} tends to be higher for long ELMs than for the short ELMs.

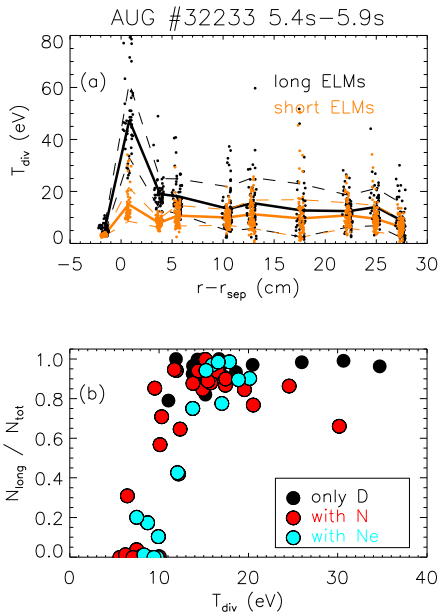

Figure 3. (a) pre-ELM T_{div} profiles for long and short ELMs from Langmuir probes. (b) Correlation between the fraction of long ELMs versus the pre-ELM T_{div}.

The analysis has been extended to three datasets in which scans of deuterium fuelling, nitrogen seeding and neon seeding were performed. The results are summarized in figure 3(b), where the correlation between the fraction of long ELMs and T_{div} is shown. The second collapse (i.e. long ELMs) is present only at high T_{div}. The trends are similar for both the nitrogen seeded and the neon seeded plasma. This suggests that the pre-ELM divertor temperature might be an important parameter for the presence of the long ELMs.

SOL DENSITY.

It was suggested in references [2,4] that the presence of the second collapse might be correlated to the high SOL density. This statement might be consistent with the fact that in TCV the long ELMs are present with high gas fuelling. In this section we investigate the SOL density in AUG and TCV. For the AUG dataset, the Li-beam is used and the SOL density is estimated using a linear fit to identify the knee at the pedestal bottom. The pre-ELM SOL density for an AUG shot is shown in figure 4(a) during a time interval where long and short ELMs co-exist. The difference is minimal, but n_e^{SOL} for the long ELMs seems slightly higher than for the short ELMs. Figure 4(b) shows n_e^{SOL} for the entire dataset (when the Li-beam was available). The range in n_e^{SOL} is quite narrow and no firm conclusion is possible. However, the result seems to suggest that no short ELMs are present at high n_e^{SOL}. The results for the TCV dataset are shown in figures 4(c) and 4(d). The Thomson Scattering has been used but, due to the lack of a clear knee, the density is estimated at the separatrix (assuming 50eV at the LCFS). The uncertainty is very large and no conclusive claims are

possible, but the discharge with highest number of long ELMs seems to be characterized by higher n_e^{sep}, approximately in agreement with the AUG result.

CONCLUSIONS.

(1) The disappearance of the second collapse is not simply correlated to high T_e^{ped} but also to high n_e^{ped} (figure 1). Hence, pedestal resistivity and collisionality do not play a role in the presence of the second collapse: the second phase disappears at low resistivity and low collisionality (for the N seeded case, with high T_e^{ped}), but also with no resistivity variation and at high collisionality (for Ne seeded case, with high n_e^{ped}).

(2) The nitrogen has no special role in the disappearance of the second collapse since also the neon can produce similar effects.

(3) The second collapse is not correlated to the pedestal pressure, as shown from figure 2(c).

(4) Short ELMs are not present at high T_{div}, regardless of the seeded species.

(5) Results seem to suggest that the short ELMs are not present in high SOL density plasma.

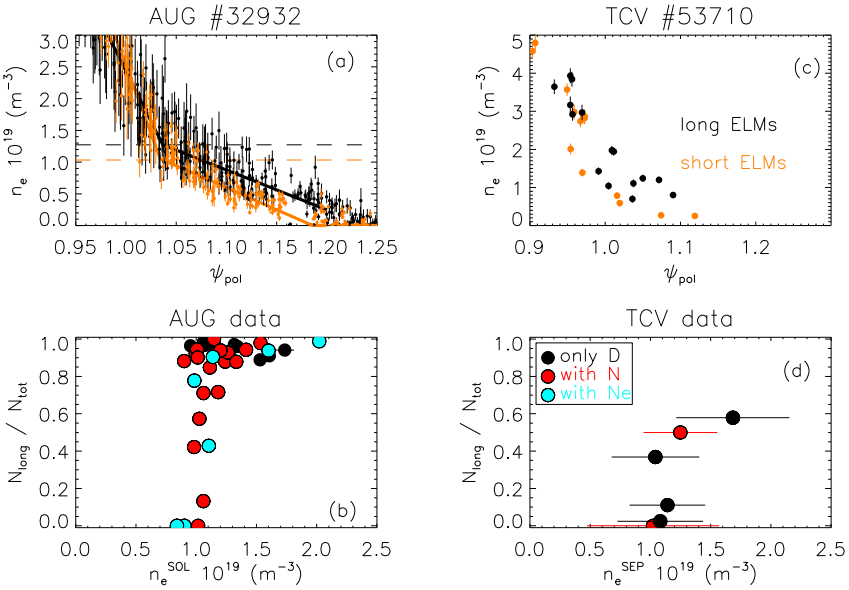

Figure 4. SOL density profile for long and short ELMs in (a) AUG (using Li-beam) and (c) TCV, using TS. Correlation between fraction of long ELMs and (b) SOL density in AUG (quantified with a linear fit) and (d) separatrix density in TCV (quantified by averaging the TS data in the range ψ=0.98-1.02).

ACKNOWLEDGEMENT.

This work has been carried out within the framework of the EUROfusion Consortium and has received funding from the Euratom research and training programme 2014-2018 under grant agreement No 633053. The views and opinions expressed herein do not necessarily reflect those of the European Commission.

REFERENCES

[1] Frassinetti L. et al., Nucl. Fusion **55**, 023007 (2015)
[2] Schneider P. et al., Plasma Physics and Control. Fusion **57** 014029 (2015)
[3] Frassinetti L. et al., Nucl. Fusion **57**, 022004 (2017)
[4] de la Luna E. et al., *"Type I ELM characterization in JET with the ITER-like wall"*, 15th H-mode Workshop, Garching (Germany) 19-21 October 2015.
[5] Schweinzer J. et al., Nucl. Fusion **51** 113003 (2011)
[6] Giroud C et al., *Plasma Phys. Control. Fusion* **57** 035004 (2015)
[7] Dunne M et al., Plasma Phys. Controll. Fusion **59** 025010 (2017)